Mat. Res. Soc. Symp. Proc. Vol. 688 © 2002 Materials Research Society

Structure and Morphology of Epitaxially Intergrown (100)- and (116)-Oriented $SrBi_2Ta_2O_9$ Ferroelectric Thin Films on $SrLaGaO_4$(110) Substrates

H. N. Lee, D. N. Zakharov, P. Reiche,[1] R. Uecker,[1] and D. Hesse
Max-Planck-Institut für Mikrostrukturphysik, Weinberg 2, D-06120 Halle/Saale, Germany
[1]Institut für Kristallzüchtung, Max-Born-Str. 2, D-12489 Berlin, Germany

ABSTRACT

$SrBi_2Ta_2O_9$ (SBT) epitaxial thin films having a mix of (100) and (116) orientations have been grown on $SrLaGaO_4$(110) by pulsed laser deposition. X-ray diffraction θ–2θ and pole figure scans, and cross-sectional transmission electron microscopy (TEM) analyses revealed the presence of two epitaxial orientations, SBT(100) || SLG(110); SBT[001] || SLG[001] and SBT(116) || SLG(110); SBT[$\bar{1}$10] || SLG[001]. By calculating the integrated intensity of certain x-ray diffraction peaks, it was established that the crystallinity and the in-plane orientation of the (100) and (116) orientation are best at a substrate temperature of 775 °C and 788 °C, respectively, and that the volume fraction of the (100) orientation at about 770 °C reached about 60%. By scanning force microscopy and cross-sectional TEM investigations we found that the *a*-axis-oriented grains are rounded and protrude out due to the rapid growth along the [110] direction, leading to a distinct difference of the surface morphology between (100)- and (116)-oriented grains.

INTRODUCTION

Ferroelectric $SrBi_2Ta_2O_9$ (SBT) belongs to the space group $A2_1am$ and has an orthorhombic structure, a = 0.5531 nm, b = 0.5534 nm, and c = 2.4984 nm at room temperature [1]. The vector of the spontaneous polarization is directed along the *a* axis (perpendicularly to the *c* axis). The growth of epitaxial films which have their spontaneous polarization along the normal to the film plane, i.e., *a*-axis oriented films, or at least pointing out of the film plane, i.e., non-*c*-axis oriented films, is desirable for applications of SBT films to ferroelectric memory devices in planar capacitor geometry. In addition, due to its highly anisotropic structure, the ferroelectric properties are also anisotropic. Epitaxial SBT films with different crystallographic orientations, therefore, allow to study the dependence of their basic properties on the orientation. (100)/(010)- and (110)-oriented SBT films have been grown on (110)-oriented MgO [2] and (100)-oriented $SrLaAlO_4$ (SLA) [3], respectively. It appears that in most cases the epitaxial growth of the SBT film and its crystallographic orientation are based on the lattice match between film and substrate. Accordingly, in order to grow *a*-axis-oriented films of high quality, the substrates (and their orientations) should be chosen in such a way that film-substrate lattice mismatches are as low as possible. In this study, we report the epitaxial growth of SBT films on (110)-oriented $SrLaGaO_4$ (SLG) single crystal substrates. (110)-oriented SLG crystals (K_2NiF_4-type tetragonal structure, a = 0.3843 nm, c = 1.268 nm [4]) provide a good lattice match for the

growth of (100)-oriented SBT films. Surprisingly, however, an intergrowth of (100)- and (116)-oriented film regions occurs [5]. Here we report on the structure and morphology of these films.

EXPERIMENTS

The SBT films were deposited by PLD using a KrF excimer laser (λ = 248 nm), operating at a repetition rate of 5 Hz with a laser energy density of 1.7 J/cm^2. A (bismuth rich) $SrBi_{2.6}Ta_2O_9$ target, 2 inch in diameter, was used. The substrate-to-target distance was fixed at 6 cm. The deposition was carried out at various substrate temperatures between 700 and 875 °C at a fixed oxygen pressure of 0.4 mbar. In order to characterize the crystallographic orientation and the epitaxial relations of the films, x-ray diffraction (XRD) θ–2θ and pole figure scans were recorded by means of a Philips X'Pert MRD four-circle diffractometer using Cu-K_α radiation and a parallel plate collimator in front of the detector implying a 2θ resolution of 0.1°. The microstructure has been investigated by transmission electron microscopy. A scanning force microscope (SFM) (Digital Instruments D5000) working in the tapping mode was used to characterize the surface morphology.

RESULTS AND DISCUSSION

Figure 1 shows an XRD θ–2θ scan of an SBT film deposited on an SLG(110) substrate at 775 °C. Upon first sight, it seems that the SBT film is entirely *a*-axis-oriented. However, as is explained below in detail, x-ray diffraction pole figures showed that a mix of (100) and (116) orientations occurs in the film and that the (116) orientation is even rather dominant under the deposition conditions used for this particular film although the recorded intensity of the 22$\underline{12}$ peak in the θ–2θ scan is rather low.

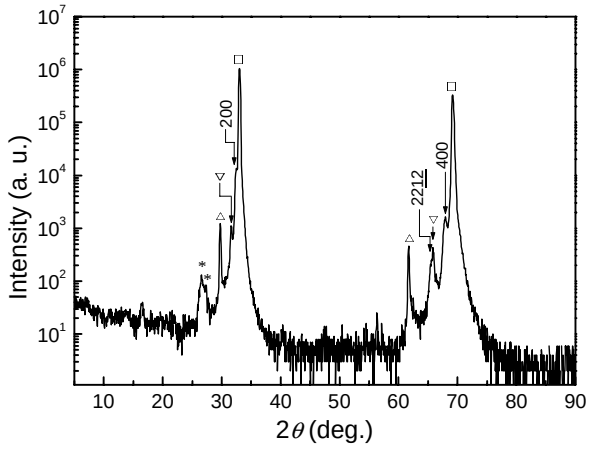

Figure 1. θ–2θ x-ray diffraction scan of an SBT film deposited on an SLG(110) substrate at 775 °C. The peaks from the substrate due to Cu-K_α, Cu-K_β, and W-L_α radiations are labeled as (□), (△), and (▽), respectively. The latter results from the tungsten contamination of the x-ray target by the tungsten cathode filament. Unidentified phases are marked (∗), which might be related to the interfacial layer between SBT and SLG (see TEM images of Fig. 3 below).

Figure 2 shows pole figures recorded with SBT reflections of (a) type 115 and (b) type 113. In Fig. 2(a), two sets of peaks can be seen, designated "A" and "B" in the figure. Set "A" appears at $\psi \approx$ 56° and consists of the 115, $1\bar{1}5$, $11\bar{5}$, and $1\bar{1}\bar{5}$ peaks from the (100)-oriented part of the film indicating that this part has a single-domain situation (ignoring *a*-*b* twins), with the SBT [001] direction aligned to the SLG [001] direction. Set

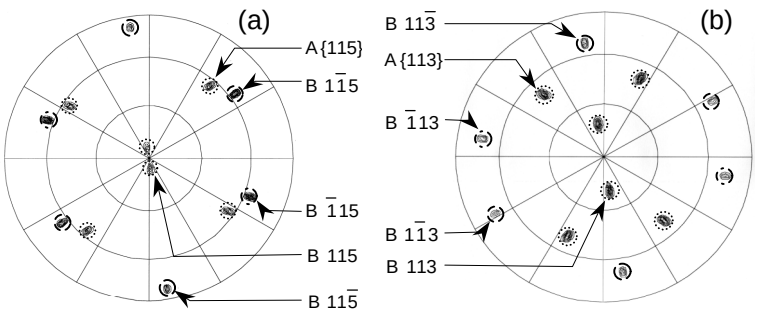

Figure 2. X-ray diffraction pole figures of the film of Fig. 1 recorded with SBT reflections of (a) type 115 and (b) type 113. Peaks originating from (100)- and (116)-oriented parts of the SBT film are denoted "A" and "B", respectively. The center and the rim of the plotted pole figures correspond to $\psi = 0°$ and 90°, respectively. $\psi = 90°$ corresponds to the substrate surface being parallel to the scattering vector.

"B" appears at $\psi \approx 5°$, 65°, and 81° and consists of the four corresponding 115, $1\bar{1}5/\bar{1}15$, and $11\bar{5}$ peaks from the (116)-oriented part of the film, which is twinned [cf. Fig. 3(b) below]. Similarly, a pole figure recorded using the 113 reflections also clearly confirms the mix of (100) and (116) orientations labeled with "A" and "B" in Fig. 2(b), respectively. Based on all these XRD results, the epitaxial orientation relationships for the (100)- and (116)-oriented parts of the film can be described as

SBT(100) || SLG(110); SBT[001] || SLG[001]
SBT(116) || SLG(110); SBT[$\bar{1}$10] || SLG[001].

Figure 3 shows cross-sectional TEM images and corresponding schematic drawings of the SBT film on the SLG(110) substrate deposited at 775 °C. Marked with arrows in the TEM image of Fig. 3(a) the [001] direction is running parallel to the substrate, which is equivalent to the epitaxy relationship SBT(100) || SLG(110); SBT[001] || SLG[001]. This relationship is illustrated in the schematic drawing, in which one unit cell of SBT is situated exactly on two underlying SLG unit cells, their *c* axes being parallel. The values of the lattice mismatch along the SBT[001] || SLG[001] and SBT[010] || [$\bar{1}$10] directions are calculated to be about 1.6% and 1.8%, respectively. Figure 3(b) shows a cross-section TEM image and the corresponding scheme for the two twins of the (116) orientation. In the schematic drawing, the SBT [001] direction is running nearly parallel to either the SLG [100] or [010] direction and is tilted about 43° out of the film plane, the SBT (116) plane being almost parallel to the SLG (110) plane. The presence of two kinds of twins has been confirmed by TEM images of the (116)-oriented part of the film (Fig. 3(b)). In this case, higher lattice misfit values of –7.5% and 5.1% along the SBT[$\bar{3}\bar{3}$1] || SLG[1$\bar{1}$0] and SBT[$\bar{1}$10] || SLG[001] directions, respectively, are calculated. However, although the TEM results confirm the XRD results of Figs. 1 and 2, some questions on the nature and origin of the interfacial layer between film and substrate seen in the TEM images arise. This layer, up to 50 nm in thickness, is most probably due to an interdiffusion and/or reaction process. Probably this process occurs after the epitaxial SBT nucleation has taken place, otherwise, the epitaxial growth based on the lattice fitting would not occur on the SLG substrate due to the presence of the interfacial layer having probably different lattice parameters. Bi atoms are a possible cause of the interface reaction or diffusion because other materials such as YBCO [6] and Sr_2RuO_4 [7] deposited on SLG and SLA at 750 °C and up to 1050 °C, respectively, did not show any significant reaction or interdiffusion. Therefore, in order to grow SBT films on SLG substrates at high temperatures, the use of a proper barrier electrode, which has a good lattice

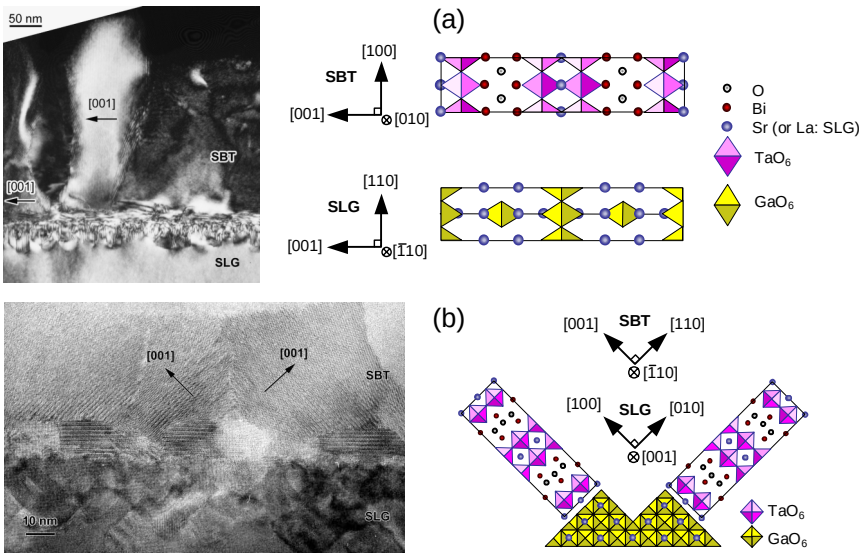

Figure 3. Cross-sectional TEM images and schematic cross-sectional projections of (a) (100)-oriented SBT on SLG(110), and (b) (116)-oriented SBT on the same substrate. Due to the double-domain (twin) situation of the (116)-oriented SBT, the SBT [001] direction is parallel to either SLG [100] or SLG [010].

mismatch with SLG, such as Sr_2RuO_4 is required to prevent the interaction at the interface keeping the orientation of the SBT films.

In view of the relatively large misfits, the presence of the (116) orientation (with the *c*-axis pointing out of the film plane) can not be simply explained considering the in-plane lattice parameters. However, as Fig. 3(b) suggests, the growth of (116)-oriented SBT on SLG(110) can also be considered as a (001)-oriented SBT growth on SLG(100) facets. This orientation would, however, be in contra-diction to the observation of Lettieri *et al.* [3], who observed that SBT grows (110)-oriented on $SrLaAlO_4$(100). (The latter substrate is most similar to SLG.) We therefore performed further growth experiments of SBT on $SrPrGaO_4$ (SPG). The crystal structure of SPG (tetragonal, a = 0.3813 nm, c = 1.2532 nm [8]) is also most similar to that of SLG. Indeed we were able to show that SBT grows on SPG(100) in the (001) orientation as shown in Fig. 4. This figure shows an XRD θ–2θ scan of an SBT film deposited on an SPG(100) substrate revealing that the SBT (001) plane is parallel to the SPG(100) substrate. The full-width at half maximum (FWHM) values of the SBT 00$\underline{1}$0 reflection are 0.41° and 0.91° in 2θ and ω scans, respectively. Considering the close similarity of SPG and SLG, the growth of the (001)-oriented SBT on (100) facets of the SLG(110) substrate is thus a possible explanation for the observed (116)-oriented growth of SBT on SLG(110).

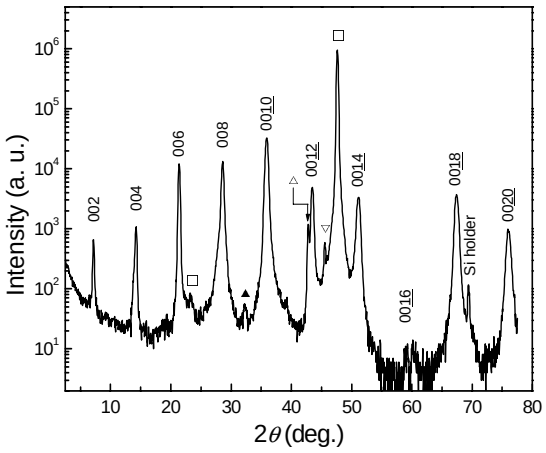

Figure 4. θ–2θ x-ray diffraction scan of a (001)-oriented SBT film deposited on an SPG(100) substrate. A peak from the SBT film due to Cu-K_β radiation is labeled as (▲). For the other symbols, see Fig. 1.

In order to check whether the (100) orientation competes with the (116) orientation in a similar way as in the case of (110)- and (103)/(013)-oriented super-

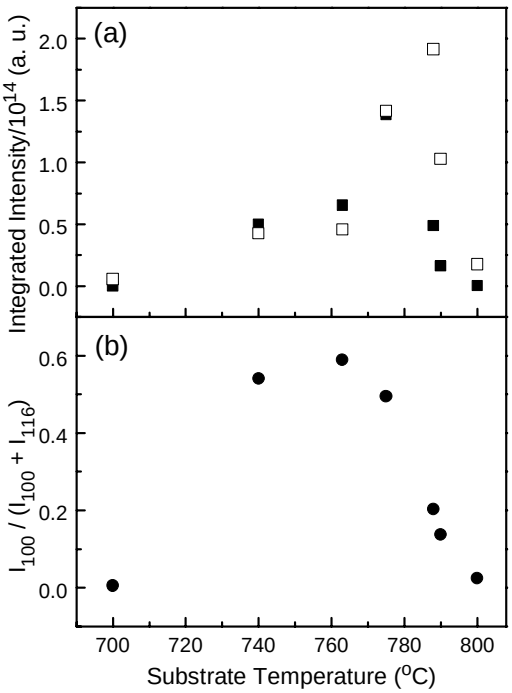

Figure 5. (a) Integrated intensities of the SBT 115 reflections from the (100)-oriented (solid squares) and (116)-oriented (open squares) film parts. (b) Calculated volume fraction of the (100)-oriented part of the film.

conducting YBCO films on $SrTiO_3$(110) [9], we have calculated integrated x-ray diffraction intensities taking into account both the intensity and the FWHM of the SBT 115 peak in θ–2θ, ϕ, and ψ scans as a function of deposition temperature. Figure 5 shows the integrated intensities of the (100)- and (116)-oriented parts of the film (a) and the fraction of the (100)-oriented part (b), $I_{100}/(I_{100} + I_{116})$, as a function of substrate temperature. For these measurements, the peaks of 115 type at $\psi \approx 56°$ and 65° have been used for the (100) and (116) orientations, respectively, since these ψ angles are close to each other. It can be concluded that the crystallinity and the in-plane orientation of the (100) and the (116) orientation reach their best values at 775 °C and 788 °C, respectively. The FWHM values of the 115 reflection corresponding to the (100)-oriented part of the film deposited at 775 °C are 0.37°, 1.9°, and 2.1° in 2θ, ω, and ψ scans, respectively. For the (116)-oriented part of the film deposited at 788 °C, these values are 0.36°, 1.0°, and 1.1°, respectively. The maximum volume fraction of the (100) orientation is about 60% in this temperature range [Fig. 5(b)]. Above 790 °C, the decreasing integrated intensity in Fig. 5(a) indicates the degradation of both these orientations and the possible presence of bismuth-deficient foreign phases due to the more significant reaction or interdiffusion between the film and substrate as well as the re-evaporation of bismuth from the film at higher temperature.

SFM studies of films deposited at 775 °C revealed distinct different morphologies between (100)- and (116)-oriented grains as shown in Fig. 6. As already reported earlier in a study of the surface morphology of (116)-oriented SBT films on (011) $SrTiO_3$ [10], the long edges of the (116) grains are parallel to SBT $[\bar{1}10]$ and the *c* axes of the grains point ~43° out of the film plane, the *c* axis being perpendicular to the long edge of the grain. In Fig. 6, referring to this morphology of (116) grains, one can readily find out the long (116)-oriented grains, which are aligning their long axes parallel to the SLG [001] direction [cf. Fig. 3(b)]. In contrast, the rounded grains in the SFM image correspond to the (100)-oriented SBT grains, which are somewhat higher than the (116) grains. It is known that the growth rate of YBCO grains along both the *a* and the *b* direction is higher than along the *c* axis [11].

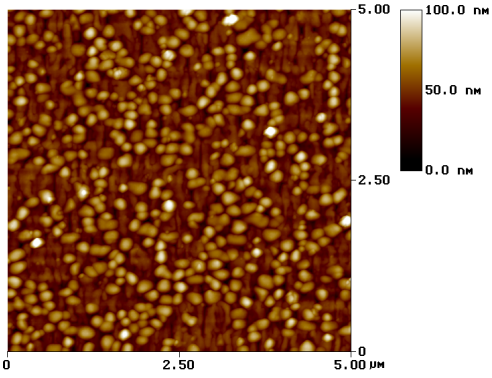

Figure 6. SFM topographic image of a mix of (100)- and (116)-oriented SBT grains.

Unlike YBCO (which has also an anisotropic structure, but $\sqrt{2} \cdot a_{\mathrm{YBCO}} \approx a_{\mathrm{SBT}}$, $\sqrt{2} \cdot b_{\mathrm{YBCO}} \approx b_{\mathrm{SBT}}$, and $2 \cdot c_{\mathrm{YBCO}} \approx c_{\mathrm{SBT}}$), plane-view TEM analyses of (110)-oriented SBT grains by Choi *et al.* revealed that the growth rate of grains along the [110] direction of orthorhombic SBT is highest or at least higher than along the *c* axis [12]. This is in good agreement with the long grains in the (116)-oriented parts of our films, in which the $[\bar{1}10]$ direction is lying in the film plane, and thus (100)-oriented grains having the [110] direction tilted 45° out of the film plane are more or less rounded.

CONCLUSIONS

In summary, we have grown SBT films with a mixed (100) and (116) orientation on (110)-oriented SLG substrates although there occurs a reacted or interdiffused layer between the film and the substrate. From integrated x-ray diffraction intensity measurements, the volume fractions of these two orientations depend on the substrate temperature, the fraction of the (100)-oriented part reaching about 60% at a temperature of about 770 °C. By SFM investigations of the mixed orientation, we have found distinct differences in the surface morphology between the (100)- and (116)-oriented grains, which can be explained assuming that SBT grains have a high growth rate along the [110] direction.

REFERENCES

1. A. D. Rae, J. G. Thompson, and R. L. Withers, Acta Crystallogr., Sect. B: Struct. Sci. **48**, 418 (1992).
2. S. E. Moon, T. K. Song, S. B. Back, S.-I. Kwun, J.-G. Yoon, and J. S. Lee, Appl. Phys. Lett. **75**, 2827 (1999).
3. J. Lettieri, Y. Jia, M. Urbanik, C. I. Weber, J-P. Maria, D. G. Schlom, H. Li, R. Ramesh, R. Uecker, and P. Reiche, Appl. Phys. Lett. **73**, 2923 (1998).
4. A. Dabkowski, H. A. Dabkowska, and J. E. Greedan, J. Cryst. Growth **132**, 205 (1993).
5. H. N. Lee, D. N. Zakharov, S. Senz, A. Pignolet, and D. Hesse, Appl. Phys. Lett. **79**, 2961 (2001).
6. S. Miyazawa and M. Mukaida, Jpn. J. Appl. Phys. **35**, L1177 (1996).
7. S. Madhaven, D. G. Schlom, A. Dabkowski, H. A. Dabkowska, and Y. Liu, Appl. Phys. Lett. **68**, 559 (1996).
8. R. Uecker, P. Reiche, S. Ganschow, D.-C. Uecker, and D. Schultze, Acta Phys. Pol. A **92**, 23 (1997).
9. See, for instance, T. Terashima, Y. Bando, K. Iijima, K. Yamamoto, and K. Hirata, Appl. Phys. Lett. **53**, 2232 (1988).
10. H. N. Lee, A. Visinoiu, S. Senz, C. Harnagea, A. Pignolet, D. Hesse, and U. Gösele, J. Appl. Phys. **88**, 6658 (2000).
11. X. K. Wang, D. X. Li, D. Q. Li, Y. P. Lu, S. N. Song, Y. H. Shen, J. Q. Zheng, R. P. H. Chang, J. B. Ketterson, J. M. Chabala, D. Hansley, and R. Levi-Setti, J. Appl. Phys. **67**, 4217 (1990).
12. J. H. Choi, J. Y. Lee, and Y. T. Kim, Appl. Phys. Lett. **74**, 2933 (1999).